

EVALUATION OF UPPER ATMOSPHERIC OZONE DATA PROVIDED BY A
DIFFERENTIAL-ABSORPTION LIDAR

A Thesis
Presented to
The Academic Faculty

By
Kimberly Kubera

In Partial Fulfillment
Of the Requirements for the Degree
Master of Science in Atmospheric Chemistry

Georgia Institute of Technology
May, 2005

EVALUATION OF UPPER ATMOSPHERIC OZONE DATA PROVIDED BY A
DIFFERENTIAL-ABSORPTION LIDAR

Approved by:

Dr. Judith Curry, Advisor
School of Earth and Atmospheric Sciences
Georgia Institute of Technology

Dr. Michael Chang
School of Earth and Atmospheric Sciences
Georgia Institute of Technology

Dr. Yuhang Wang
School of Earth and Atmospheric Sciences
Georgia Institute of Technology

Date Approved: April 7, 2005

ACKNOWLEDGMENTS

I would like to make an acknowledgment of appreciation to those who have given me special assistance. These people whom I would like to recognize are Dr. Michael Chang, Dr. Judith Curry, Dr. Yuhang Wang, Dr. Gary Gimmestad and the GTRI researchers, and Ms. Susan Ryan.

TABLE OF CONTENTS

ACKNOWLEDGEMENTS	iii
LIST OF TABLES	v
LIST OF FIGURES	vi
SUMMARY	vii
CHAPTER 1 INTRODUCTION	1
Regulations and Health Impacts	1
Ozone Formation	3
Impact of the Mixing Layer on Ozone Concentrations	5
NEXLASER	7
CHAPTER 2 METHODS	12
Early Morning Upper-Tropospheric Ozone Layers	12
Mixing Height Analysis	13
NEXLASER and Surface Comparisons	16
CHAPTER 3 RESULTS	19
CHAPTER 4 CASE STUDIES	27
Case 1: 2 August through 5 August	29
Case 2: 17 August through 20 August	36
CHAPTER 5 CONCLUSION	44
REFERENCES	45

LIST OF TABLES

Table 1	Ozone layers	13
Table 2	Weather observations adjusted to numeric values for surface and opaque cloud coverage	16
Table 3	Study days	18
Table 4	R-squared values between layers for each hour	19
Table 5	Standard deviations within each layer	24
Table 6	Correlations between upper-tropospheric ozone and surface 8-hour ozone maximums	25
Table 7	Maximum 8-hour average ozone per monitoring site and rate of ozone increase (2 August – 5 August)	34
Table 8	Maximum 8-hour average ozone per monitoring site and rate of ozone increase (17 August – 20 August)	41

LIST OF FIGURES

Figure 1	Schematic of diurnal process	6
Figure 2	Laser diagram	8
Figure 3	Ozone and sulfur dioxide absorption cross-sections with regularly used wavelengths marked by vertical lines	11
Figure 4	Atlanta map	17
Figure 5	Ozone concentrations and corresponding hourly mixing heights for 27 August 2004	22
Figure 6	Ozone concentrations and corresponding hourly mixing heights for 26 August 2004	23
Figure 7	Metropolitan Atlanta's daily maximum ozone concentration	27
Figure 8	2 August Meteogram	29
Figure 9	3 August Meteogram	30
Figure 10	4 August Meteogram	31
Figure 11	5 August Meteogram	32
Figure 12	NEXLASER and hourly mixing height charts for 2 August through 5 August	33
Figure 13	17 August Meteogram	36
Figure 14	18 August Meteogram	37
Figure 15	19 August Meteogram	38
Figure 16	20 August Meteogram	39
Figure 17	NEXLASER and hourly mixing heights for 17 August through 20 August	40

SUMMARY

Ground-level ozone is an environmental and public health issue. Daily ozone forecasts are made to allow people to take precautions to protect their health. For this study, a prototype laser that measures ozone concentrations vertically throughout the atmospheric boundary layer was evaluated as tool for ozone forecasting.

To examine this data, three analyses were performed. First, it was determined if stratification, and thus residual layers, could be seen. This was conducted, in part, by examining hourly mixing heights overlaid onto color-coded NEXLASER charts. Each NEXLASER chart shows the horizontal and spatial distribution of the measured ozone concentrations during a twenty-four hour period. In the second analysis, the correlation value between the early morning upper-tropospheric ozone and the maximum 8-hour average surface ozone concentrations was determined. For the third analysis, a case study on two select groups of days was conducted.

This study suggested that NEXLASER can be used to detect the presence of residual layers and can be used as an aid in predicting peak daily 8-hour average ground-level ozone concentrations. Specifically, days on which a morning ozone reservoir layer is most prominent have the most potential to lead to high surface ozone concentrations later in the day. While more research should be conducted, this study shows how this data could be useful in explaining ozone events, and thus be an aid to ozone forecasters.

CHAPTER 1

INTRODUCTION

Ground-level ozone is an environmental and public health issue. Because of health concerns associated with exposure to high concentrations of ozone, it is desirable to provide accurate forecasts of future ozone concentrations as far in advance as possible. The primary goal of ozone forecasts, now offered in many communities, is to provide the public in general, and those that are susceptible to ozone in particular, sufficient warning such that people may take precautions to limit or avoid exposure, and as a consequence, improve health outcomes. For this study, a prototype laser that measures ozone concentrations vertically throughout the atmospheric boundary layer was evaluated as tool for ozone forecasting.

Regulations and Health Impacts

The main focus of ozone forecasts is to provide the public with advance warning of ozone concentrations so that individuals can take precautions to protect their health. This is in addition to the United States Environmental Protection Agency's (U.S EPA) continuing effort to protect human health from the adverse effects of ozone since it was authorized to set pollutant standards within the Clean Air Act in 1970. The standards within this Act are periodically re-evaluated using the latest scientific research. In 1997, the EPA replaced the 1-hour primary standard for ozone with a new 8-hour standard based on review of available scientific evidence documenting the adverse health effects due to ozone exposure. In their last review of health impacts related to ozone exposure, the EPA cited studies showing decreases in lung volume and inflammation of respiratory

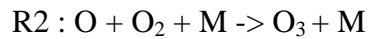
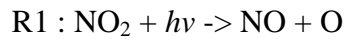
tissues, evidence related to response and recovery times, and health exacerbations related to exposures to ozone mixed with other pollutants. (U.S EPA, 1996).

The new 8-hour standard is 0.08 parts per million (ppm). A monitor is attaining the standard when the average over a three year period of the annual fourth highest daily 8-hour average ozone concentration is less than or equal to 0.084ppm. A region is attaining the standard when all monitors in the area are attaining the standard. (Federal Register, 1997; Federal Register, 2003)

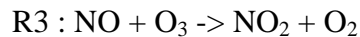
Recently, Brunekreef and Holgate (2002) reviewed current studies on the health effects of air pollutants and used a large experimental database to verify that ozone has significant biological effects at ambient concentrations. Frischer et al (2001) found that ozone exposure in healthy children is also harmful, with ozone associated with eosinophil inflammation in the airways. Long-term exposure to ozone is documented to decrease respiratory function in adults and children, whether over several hours or over a season (Kinney and Lippmann, 2000). Persistent ozone effects have also been shown to exist, especially in the day following exposure (Brauer and Brook, 1997). It also has been documented that both healthy and asthmatic individuals can develop a tolerance to daily ozone (Gong et al, 1997). However, Jorres et al (2000) determined that airway inflammation persists after repeated exposure to ozone, despite attenuation of some inflammatory markers. Reviews of recent studies have even found that adverse health effects can be seen at lower concentrations than previously thought and premature mortality effects of ozone pollution have been under predicted. (Brunekreef and Holgate, 2002; Thurston and Ito, 2001).

Ozone Formation

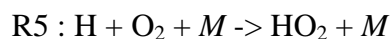
Ozone is formed from photochemical reactions between NO_x and various hydrocarbons, where the main anthropogenic source of NO_x is fossil fuel combustion, such as automobile exhaust. Anthropogenic sources of hydrocarbons include combustion, fuel evaporation, solvent use and chemical manufacturing. The reactions that produce tropospheric ozone are: (Jacob, 1999)



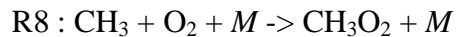
However, the key destruction mechanism of O_3 consists of the oxidation of NO to form NO_2 .



Reactions of CO , CH_4 and hydrocarbons in the presence of NO_x will produce additional NO_2 without the destruction of O_3 , thus allowing for a net increase in O_3 . Examples of these reactions are the following:



and



Both examples show how a peroxy radical is formed (HO_2 and CH_3O_2) and a subsequent oxidation of NO to NO_2 , leading to ozone production through reactions R1 and R2.

(Jacob, 1999; Pryor and Steyn, 1995; Seinfeld and Pandis, 1998; Guicherit and Roemer, 2000)

Synoptic meteorology influences the amount of ozone that is formed and where it is transported. High concentrations of ozone occurs more frequently on days occur that are sunny, hot, dry, winds are light or calm, and there is a strong temperature inversion - conditions associated with high-pressure systems. Since solar radiation activates the reactions that form ozone, more available sunlight leads to increased production of ozone. Many of the reactions above are also temperature dependent, where the higher the temperatures, the more rapid are the chemical reaction rates, and thus, ozone production. If winds are light or calm, ozone precursors will accumulate rather than disperse.

(Seinfeld and Pandis, 1998; Comrie and Yarnal, 1991) Ozone formation and accumulation is less likely to occur under meteorological conditions associated with low-pressure systems. Convective and upward motions associated with fronts and cyclones vent and disperse the pollutants, and pollutant precursors, into the upper troposphere. Pollutants are also scavenged by clouds and rain and are wet-deposited to the surface.

(Arya, 1999)

Impact of the Mixing Layer on Ozone Concentrations

Pollutant dispersion is largely dependent on the height of the mixed layer that is located within the atmospheric boundary layer. The mixed layer is a layer in which compounds are homogeneously mixed through convection and turbulence. The mixed layer is capped by a temperature inversion that acts as a barrier to ground-level pollutant dispersion. An inversion is an increase in potential temperature with height. In the troposphere, potential temperatures normally decrease with height.

A nocturnal surface inversion can develop after sunset as the ground cools by radiative cooling. In the morning, the inversion is destroyed from the bottom to the top by the ground reheating due to incoming solar radiation. The mixed layer grows until the inversion eventually dissolves by midday. Below the surface inversion layer, pollutants are trapped and become well mixed by wind and turbulence. (Arya, 1999)

A subsidence inversion aloft can form as a result of sinking air associated with high-pressure systems, where the subsiding air is being heated by adiabatic compression. The entrainment of pollutants by the subsidence inversion can also result in high concentrations of ozone. This is one of the reasons extreme ozone events are associated with high-pressure systems. (Arya, 1999; Baumbach and Vogt, 2003) A schematic of this diurnal process is shown in Figure 1.

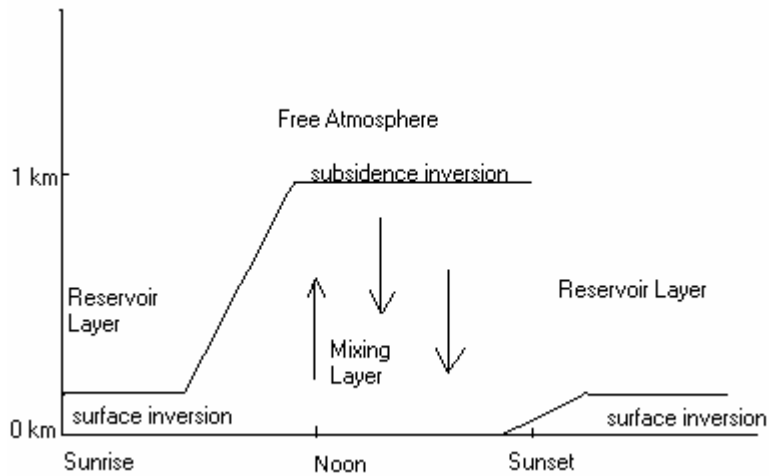


Figure 1: Schematic of diurnal process

Studies such as the one conducted by Hayden et al (1997) and Ludwig et al (1995), have shown that the mixed layer depth has a significant effect on ozone concentrations. Hayden et al studied the boundary layer structure in the Lower Fraser Valley of coastal British Columbia and found that when the ozone concentrations were high, the mixed layer depth was relatively low at 500-800m. Ludwig et al noted that high-ozone concentrations at Pinnacles National Monument, in northern California, occurred on days with shallow mixing layers and strong inversions. Their analysis also suggests that the winds and stable inversion layers cause the ozone violations in that region.

The correlation of the mixing layer height and ozone concentrations was used by Cox and Chu (1993) to model ozone trends. They used graphical and regression methods to determine which meteorological variables are the most highly related to the daily maximum ozone concentrations. By using step-wise regression analysis and scatter plots, they found that morning mixing heights, among five other variables, best explain the

variability in maximum ozone. They also found that afternoon mixing height is a good predictor of ozone concentrations in urban centers in the western US.

Besides the direct trapping that inversions have on pollutants and pollutant precursors, inversions may also contribute to pollutant concentrations through the creation of a residual layer. At night, a lightly mixed layer that is located between the nocturnal surface inversion and the upper level subsidence inversion. This layer can contain the residual ozone formed during the previous day. Since NO_x , which is emitted at or near the surface and is the main ozone-destroying compound, cannot enter this layer due to the capping of the nocturnal surface inversion, any ozone in this layer is preserved. When the nocturnal surface inversion dissolves later in the day, ozone from the 'reservoir' can be mixed down and added to the ozone formed through photochemical processes. (Baumbach and Vogt, 2003)

NEXLASER

A lidar (Light Detection And Ranging) is an instrument that transmits and receives ultraviolet, visible or infrared light, where a laser is the transmitter and a telescope, with a given field of view, is the receiver. The laser releases a pulse of light, at a specific wavelength. This light may be reflected, refracted or absorbed by the atmosphere. The receiver measures the amount of light that is backscattered against time. Once the light is emitted, a timer starts, only to stop when light is received back. Thus, the pulse allows the distance to the gas of interest to be determined, since both the time span and speed of light are known. When the telescope receives the backscattered light, it directs it to a detector where the photons of light are converted into an electrical signal.

This electric signal is then transformed into the desired data signal. (Sica, 1999) A diagram of the basic lidar is shown in Figure 2.

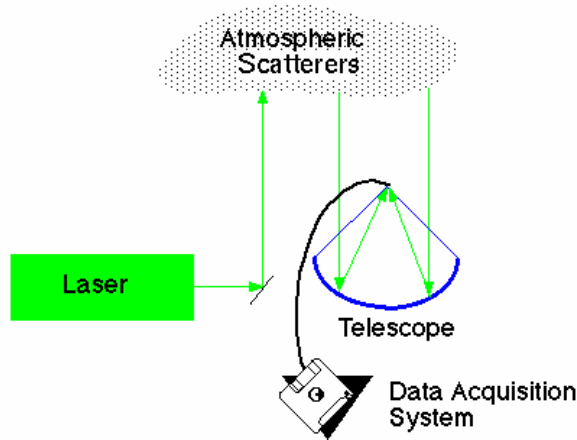


Figure 2: Laser diagram (Sica, 1999)

DIAL (Differential Absorption Lidar) is a lidar system that has two laser wavelengths that are used to measure gases in the atmosphere. One of the wavelengths is strongly absorbed by the gas while the second is absorbed to a lesser extent. The two wavelengths are emitted into the atmosphere and are scattered back to two receivers. (Vaughan, 2003) The following basic elastic backscatter lidar equation is used by the DIAL system to calculate the received signal strength:

$$P(R) = P_0 \eta (A/R^2) (c\tau/2) \beta(R) \exp[-2 \int_0^R \alpha(R) dr]$$

In this equation, $P(R)$ represents the power, or amount of photons, received at range R and P_0 is the average power transmitted throughout the laser pulse. The receiver

efficiency is represented by η , the receiver area by A , and the distance to the scattering volume by R . The speed of light is represented by c , and τ is the duration of the laser pulse. Finally, the atmospheric backscatter coefficient and the atmospheric extinction coefficient are represented by β and α , respectively. They depend on the two chosen wavelengths, λ_{on} and λ_{off} , and have a separate value for each wavelength. These wavelengths have different absorption cross-sections, as previously mentioned, and correspond to signals P_{on} and P_{off} . Using these two signals, along with additional variables such as the change in absorption cross-sections and wavelength dependent correction terms based on extinction coefficients, the number density of the measured gas can be determined. Once the number density is determined, the concentration can be calculated. (Gimmestad, 2005)

DIAL systems have been extensively studied. Fredriksson and Hertz (1984) and Weibring et al (2003) studied using these instruments to measure different gases and fitting them into mobile vans. The National Oceanic and Atmospheric Administration (NOAA) built a mobile DIAL van known as OPAL (Ozone Profiling Atmospheric Lidar) (Gimmestad, 2005) While much of the DIAL technology is well known, there are still issues that need to be taken into consideration. For example, when two wavelengths are emitted, a systematic error occurs if one of the two wavelengths has a different overlap with the field of view than the other. Also, the DIAL equation, mentioned previously, will assume that the signals received are constructed of single-scattering events if corrections are not made. This is important in turbulent atmospheres, where several scattering events will contribute to the signals. Again, this can cause systematic errors

(Fredriksson and Hertz, 1984). Sasano et al (1985) explains in detail the errors that can occur when determining the extinction and backscattering coefficients.

Researchers at the Georgia Tech Research Institute (GTRI) are constructing and testing a new prototype DIAL, called NEXLASER, which builds upon the already existing DIAL technology and is used to measure upper-atmospheric ozone. Specifically, NEXLASER is proposed as an unattended network of DIAL systems that will be simpler to operate, more reliable, produces real-time reduced data, has eye safety, uses standard measurement techniques and is generally lower in cost. (Gimmestad, 2005)

Because the NEXLASER system utilizes the ultraviolet (UV) spectrum, wavelengths that absorb ozone within that region must be chosen. Using the UV spectrum is important because several pollutants that are key for urban air studies have spectra in that zone. Also, eye safety requirements can be met and the sky background radiance is small. Figure 3 depicts the UV spectrum's ozone and sulfur dioxide absorption cross-sections, along with vertical lines that represent three regularly used DIAL wavelengths. The NEXLASER uses the 289nm/299nm DIAL pair to measure ozone. Sulfur dioxide is depicted in Figure 3 because it can act as an interfering gas at certain wavelengths. (Gimmestad, 2005)

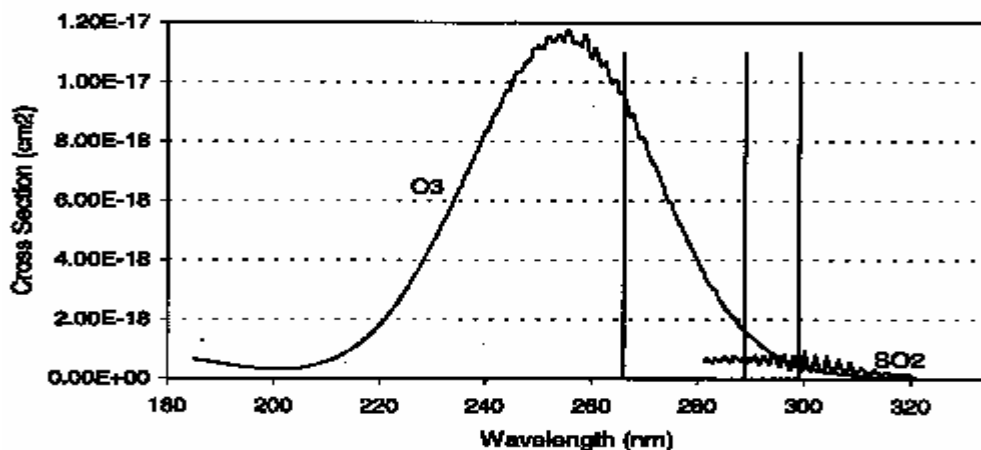


Figure 3: Ozone and sulfur dioxide absorption cross-sections with regularly used wavelengths marked by vertical lines. (Gimmestad et al, 2001)

NEXLASER was designed to keep errors in ozone concentration below 10ppb. The allowed errors are partitioned such that statistical errors in ozone concentration are kept below 7ppb when 2500 pulses are averaged. As for systematic errors, the remaining 3ppb includes uncertainty in absorption cross-sections and residual aerosol correction terms, the latter which are used to help take into account such things as interfering gases. However, the influence of SO_2 and NO_2 is not considered in the construction of NEXLASER. These are relevant when applying the wavelengths used by the instrument and thus can lead to additional errors. (Stewart et al, 2002)

Even given the inherent errors, DIAL technology has been shown to measure ozone profiles with reasonable accuracy and NEXLASER seeks to improve upon it. However, the purpose of this study is not to validate the instrument but examine whether data collected from it can be used to explain surface ozone concentrations. In particular, the hypothesis of this study is that NEXLASER can be used to detect the presence of residual layers and can be used as an aid in predicting peak daily ground-level ozone concentrations.

CHAPTER 2

METHODS

Hourly concentrations of ozone collected using NEXLASER during the summer of 2004 in Atlanta, Georgia were examined in this study. Specifically, this information was retrieved from the roof of the Baker Building on the Georgia Institute of Technology campus (33.46 N and 84.23 W).

NEXLASER collected ozone concentrations throughout the lower and upper troposphere approximately every 2 minutes. A 1-hour average concentration was calculated for each hour by aggregating the 2-minute data. These averages were stored at the beginning of the hour. For example, the 9am average is for all measured values between 9am and 10am. A minimum of one 2-minute value was required for the hourly concentration; otherwise the hourly average was reported as missing. The hourly average was used for this study. NEXLASER measurements began at an altitude of 345m and continued every 15m until approximately 4000m, or until clouds were met.

Early Morning Upper-Tropospheric Ozone Layers

The main objective of this study is to see if NEXLASER data can be used to detect the presence of residual layers and examine whether this data can be used as an aid in predicting peak daily 8-hour average ground-level ozone concentrations. To accomplish this, potential stratification of the early morning upper-tropospheric data needed to be identified and correlations with surface maximum 8-hour average ozone concentrations needed to be calculated. To determine if the early morning ozone

concentrations are stratified, layers were first arbitrarily chosen. Each layer is approximately 285m in height. These layers can be seen in Table 1.

Table 1: Ozone layers

	Layer (m)
A	345-585
B	600-885
C	900-1185
D	1200-1485
E	1500-1785
F	1800-2085
G	2100-2385
H	2400-2685
I	2700-2985
J	3000-3285
K	3300-3285
L	3600-3885
M	3900-4185
N	4200-

Correlations between these layers of average hourly ozone concentrations were calculated to determine the relationship between the layers. If the calculated correlations were weak, then the layers are sufficiently different, suggesting that ozone is stratified within the boundary layer (as opposed to well mixed).

Mixing Height Analysis

Since showing if ozone reservoir layers exist and if they impact afternoon surface ozone maximum concentrations is key for this study, it is important to see how and when this layer intersects the mixing layer. In order to see this, diurnal mixing heights were

determined using programs made publicly available by the EPA and plotted over NEXLASER ozone charts. Each NEXLASER chart was a color-coded spatial plot of all the 2-minute measurements made for that day and was constructed by the GTRI researchers. The programs used in this analysis to estimate the hourly mixing heights were the Mixing Height Program and PCRammet (U.S EPA, 2005).

The first of these programs determined the daily minimum and maximum mixing heights. Mixing heights are determined using temperature profiles, which National Weather Service (NWS) radiosondes provide daily at 0Z and 12Z. For this study, the radiosonde data was retrieved through the Radiosonde Database Access webpage, which is produced with the National Oceanic and Atmospheric Administration (Govett, 2001). This data was for Peachtree City (33.4 N, 84.6W), the site closest to the NEXLASER site at Georgia Tech. The basics of determining the two mixing heights from these profiles involve the temperature and pressure at the surface and in the upper atmosphere. These numbers are used to calculate the potential temperature with height. For each level examined, the potential temperature aloft is compared to the surface air. If the potential temperature at that level is less than that of the surface, the air will continue to rise. This is because warm air is less dense than cold air. Once a level is found where the potential temperature aloft is greater, that is where the top of the mixing layer is defined. This process is repeated for both the 0Z and 12Z soundings, resulting in the daily minimum and maximum mixing heights. (U.S EPA, 1990)

Once these values are calculated, the PCRammet program is used to estimate the hourly mixing heights. This program requires mixing height data determined using the Mixing Height Program along with hourly surface observations. It takes the morning and

afternoon mixing heights from the previous day, the current day, and the following day and interpolates the hourly values between them by using hourly estimates of stability. To estimate the stability, Turner's insolation classes and Pasquill-Gifford stability classes are applied. These classes depend upon daytime insolation, nighttime cloudiness and surface wind speed. The daytime insolation is determined by cloudiness, ceiling height and solar angle. (U.S EPA, 1999) During daylight hours, light winds and strong insolation produce more unstable conditions (Arya, 1999). In nighttime, neutral conditions prevailed with less cloud coverage and lighter winds (Arya, 1999). Depending on whether the atmosphere is stable, unstable or neutral will determine between which mixing heights the interpolation occurs. For instance, if the atmosphere is neutral between midnight and sunrise, the interpolation for those hours is between the maximum mixing height value of the previous day and the maximum value for the current day. Each day is broken into similar interpolation sections. (U.S EPA, 1999) The surface data required for this program was taken from the unedited local climatological database, which was accessed through the National Climatic Data Center (NCDC) website (NCDC, 2004). Because there was incomplete data for Peachtree City for the days examined in this study, surface observations were taken from Atlanta Hartsfield-Jackson Airport (KATL). This data was measured at the end of each hour, at Local Standard Time (LST). Even from this data, assumptions had to be made. The EPA programs required numeric values for surface coverage and opaque cloud coverage. Since the data that was retrieved did not have those specific variables, adjustments were made. For those two categories, the 'weather' information obtained was used to fill those missing values. These adjustments can be

seen in Table 2. It was assumed that surface coverage and opaque cloud coverage were equal.

Table 2: Weather observations adjusted to numeric values for surface and opaque cloud coverage

Weather Observation	Surface and Opaque Cloud Coverage
CLR	0
FEW	0
SCT	0.3
BKN	0.8
OVC	1

NEXLASER and Surface Comparisons

Once stratification, and thus reservoir layers, were suggested to be present, standard deviations of the hourly ozone within the layers previously examined were calculated to determine the appropriate maximum layer to correlate with the surface ozone. If a layer had a large standard deviation then it was assumed that the NEXLASER was unable to measure that layer with enough accuracy to allow for further examination.

After a cut-off layer was determined, each morning hourly average of ozone within that layer was correlated with the afternoon maximum 8-hour ozone concentration. This correlation was calculated to determine if the early-morning upper-tropospheric ozone concentrations affected the afternoon maximum surface concentration. Morning hours were used because those are the times when a potential residual layer can be seen before it combines with the growing mixing layer. The surface maximum was determined using three arbitrarily chosen criteria utilizing the 11 different ozone-measuring sites across metropolitan Atlanta. Thus, for each hour and layer, there are three different

correlations examined. The first maximum was the highest 8-hour concentration at any of the 11 sites. The second was the average of the 11 maximum values for the region and the third was the maximum at the Confederate Avenue measuring site, which is the closest site to the Georgia Tech Campus. These concentrations were retrieved from Atlanta's ambient monitoring program air quality database (Zimmer-Dauphinee, 2005). As with the NEXLASER averages, these were recorded at the beginning of the hour. Figure 4 shows a map indicating the location of each of the monitoring sites, Peachtree City, Georgia Tech and the Atlanta Hartsfield-Jackson Airport. The days that were used in this study can be seen in Table 3. These were the days that NEXLASER could be run and spanned from mid-July through the end of September.

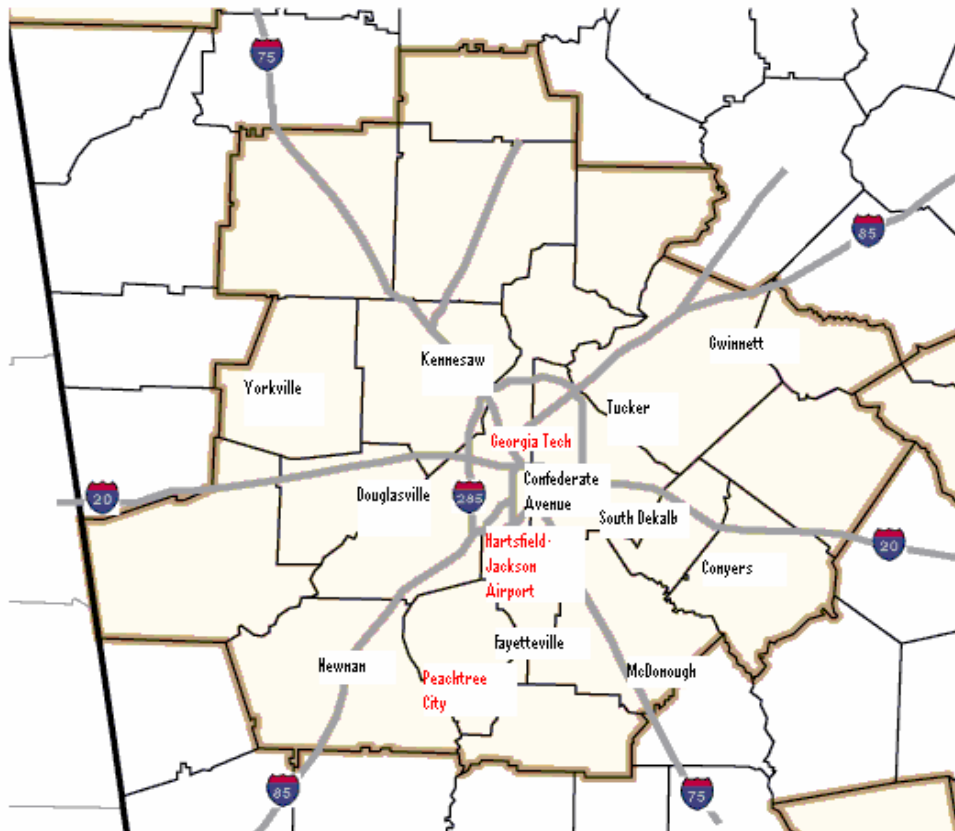


Figure 4: Atlanta map

Table 3: Study days

13-Jul	9-Aug	2-Sep
14-Jul	10-Aug	3-Sep
15-Jul	11-Aug	9-Sep
19-Jul	13-Aug	10-Sep
20-Jul	16-Aug	13-Sep
21-Jul	17-Aug	17-Sep
23-Jul	18-Aug	20-Sep
28-Jul	19-Aug	21-Sep
29-Jul	20-Aug	24-Sep
30-Jul	23-Aug	25-Sep
2-Aug	24-Aug	28-Sep
3-Aug	27-Aug	29-Sep
4-Aug	30-Aug	30-Sep
5-Aug	31-Aug	
6-Aug	1-Sep	

CHAPTER 3

RESULTS

The first question examined was if the early morning upper-tropospheric ozone was stratified. When examining the correlation between the layers, a difference can be seen. Table 4 contains the measured R-squared values.

Table 4: R-squared values between layers for each hour

6AM									
	A	B	C	D	E	F	G	H	I
I	0.045	0.046	0.301	0.475	0.101	0.244	0.022	0.231	1.000
H	0.127	0.038	0.261	0.390	0.454	0.305	0.001	1.000	
G	0.011	0.004	0.179	0.003	0.050	0.023	1.000		
F	0.475	0.642	0.896	0.725	0.275	1.000			
E	0.177	0.225	0.273	0.516	1.000				
D	0.444	0.532	0.653	1.000					
C	0.449	0.610	1.000						
B	0.822	1.000							
A	1.000								
7AM									
	A	B	C	D	E	F	G	H	I
I	0.065	0.099	0.170	0.075	0.001	0.006	0.047	0.041	1.000
H	0.007	0.030	0.026	0.015	0.029	0.019	0.398	1.000	
G	0.039	0.075	0.048	0.089	0.161	0.037	1.000		
F	0.018	0.073	0.104	0.460	0.668	1.000			
E	0.058	0.151	0.261	0.659	1.000				
D	0.221	0.354	0.683	1.000					
C	0.383	0.501	1.000						
B	0.550	1.000							
A	1.000								
8AM									
	A	B	C	D	E	F	G	H	I
I	0.023	0.072	0.088	0.199	0.040	0.086	0.082	0.136	1.000

Table 4: R-squared values between layers for each hour (continued)

H	0.017	0.115	0.144	0.589	0.256	0.367	0.822	1.000	
G	0.002	0.085	0.245	0.696	0.279	0.336	1.000		
F	0.004	0.004	0.022	0.226	0.857	1.000			
E	0.005	0.015	0.005	0.231	1.000				
D	0.083	0.179	0.483	1.000					
C	0.392	0.410	1.000						
B	0.511	1.000							
A	1.000								
9AM									
	A	B	C	D	E	F	G	H	I
I	0.050	0.117	0.124	0.210	0.175	0.244	0.303	0.505	1.000
H	0.018	0.082	0.238	0.367	0.518	0.590	0.628	1.000	
G	0.011	0.146	0.514	0.748	0.773	0.859	1.000		
F	0.033	0.143	0.548	0.799	0.916	1.000			
E	0.029	0.189	0.564	0.830	1.000				
D	0.041	0.247	0.763	1.000					
C	0.056	0.406	1.000						
B	0.262	1.000							
A	1.000								
10AM									
	A	B	C	D	E	F	G	H	I
I	0.012	0.001	0.003	0.194	0.285	0.210	0.248	0.224	1.000
H	0.093	0.273	0.213	0.372	0.529	0.521	0.492	1.000	
G	0.015	0.130	0.458	0.694	0.648	0.772	1.000		
F	0.032	0.108	0.502	0.804	0.774	1.000			
E	0.030	0.110	0.569	0.873	1.000				
D	0.070	0.120	0.731	1.000					
C	0.206	0.189	1.000						
B	0.185	1.000							
A	1.000								
11AM									
	A	B	C	D	E	F	G	H	I
I	0.002	0.093	0.000	0.128	0.095	0.380	0.298	0.507	1.000
H	0.000	0.011	0.000	0.101	0.123	0.158	0.254	1.000	

Table 4: R-squared values between layers for each hour (continued)

G	0.005	0.012	0.345	0.795	0.603	0.866	1.000		
F	0.016	0.092	0.502	0.867	0.600	1.000			
E	0.001	0.000	0.444	0.767	1.000				
D	0.020	0.080	0.632	1.000					
C	0.052	0.213	1.000						
B	0.292	1.000							
A	1.000								
NOON									
	A	B	C	D	E	F	G	H	I
I	0.060	0.171	0.003	0.163	0.138	0.099	0.045	0.442	1.000
H	0.012	0.000	0.001	0.176	0.236	0.098	0.001	1.000	
G	0.021	0.000	0.058	0.043	0.014	0.001	1.000		
F	0.234	0.135	0.444	0.514	0.781	1.000			
E	0.200	0.101	0.226	0.431	1.000				
D	0.139	0.053	0.306	1.000					
C	0.196	0.260	1.000						
B	0.171	1.000							
A	1.000								

As seen, the correlation values vary and they generally decrease as the distance between the layers increases. Thus, there is enough to suggest stratification.

This difference can further be seen when examining the NEXLASER and hourly mixing height charts. These charts were able to show in a broad approach how early morning upper-tropospheric ozone is at times stratified before it enters the mixed layer and how a potential influence on afternoon surface maximum concentrations can be suggested. However, the weather was different for each study day. Since atmospheric conditions not only influence how the mixing height evolves but also the amount of ozone formed and its dispersion, these charts displayed varying results. Figure 5 is an example of a day when there is no apparent reservoir layer, and thus no significant

stratification. Since there is no influx of high upper-tropospheric ozone concentrations, afternoon surface concentrations are probably largely due to recent chemical reactions. In contrast, Figure 6 shows an example where a potential reservoir layer and its influence can be suggested. A layer of higher ozone concentration can be seen crossing into the rising mixing height between 7am and 9am. Once this layer is mixed with the ozone formed at the surface, it can be hypothesized that this process results in a higher surface maximum. These findings validate more focused examination.

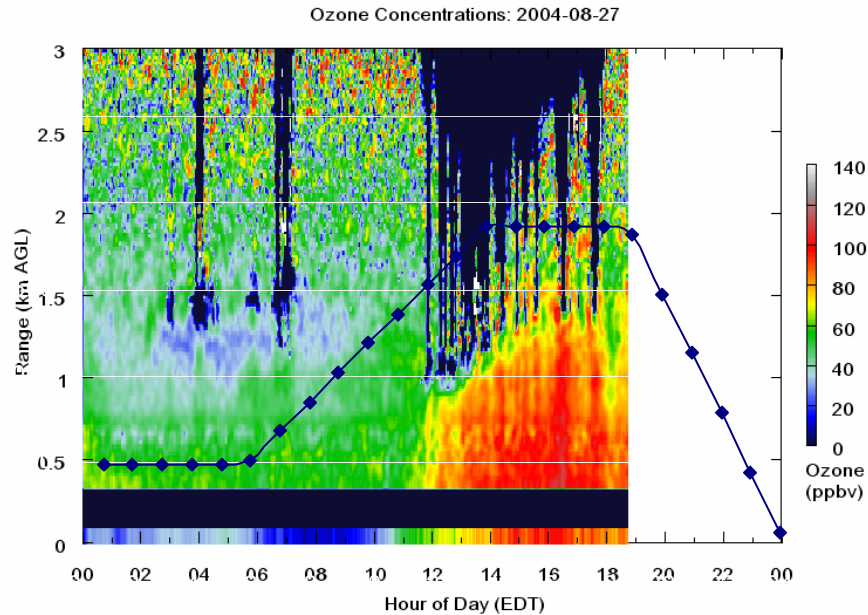


Figure 5: Ozone concentration and corresponding hourly mixing heights for 27 August 2004

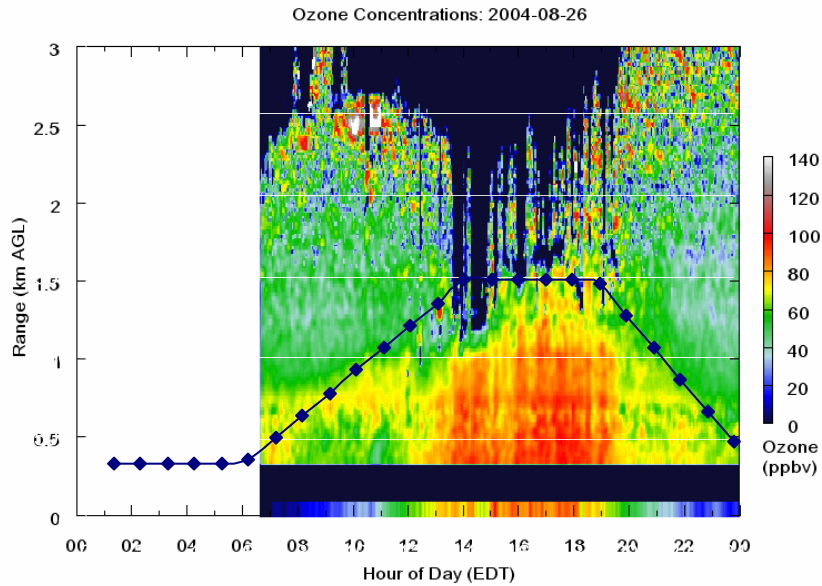


Figure 6: Ozone concentration and corresponding hourly mixing heights for 26 August 2004

Once it was determined that there is layering, the standard deviations within the layers were calculated for each study day. The average of these standard deviations was then taken such that the average standard deviation for each layer over the entire study period could be examined. These values enabled a cut-off layer to be determined. If the standard deviation was large, that means that the ozone values within that layer had a large variation. This would likely mean that the NEXLASER was not measuring accurately. Thus, further examination of that layer, and any layer above it, should not occur. Table 5 contains the calculated standard deviations.

Table 5: Standard deviations within each layer

LAYER	6:00 AM	7:00 AM	8:00 AM	9:00 AM	10:00 AM	11:00 AM	NOON
A	6.738	8.774	10.397	9.702	7.452	6.704	6.425
B	9.993	11.656	10.224	10.653	11.676	12.365	14.868
C	7.346	7.958	9.179	8.998	11.285	14.319	15.173
D	6.457	9.050	8.914	8.280	9.372	9.879	19.977
E	11.603	14.712	11.203	11.615	10.966	12.423	20.286
F	16.707	17.364	13.628	14.512	16.325	15.274	21.152
G	18.518	19.299	15.007	15.966	17.592	17.140	21.999
H	25.818	27.448	19.811	21.754	21.342	19.545	21.870
I	25.045	26.837	24.517	24.988	21.314	25.597	26.752
J	25.696	24.870	25.393	24.377	27.192	29.732	26.893
K	26.350	28.797	23.555	29.679	33.407	29.220	32.843
L	27.851	26.991	29.991	29.804	31.588	36.529	37.383
M	28.381	39.799	34.757	36.991	37.579	40.106	43.289
N	18.713	32.174	40.186	42.059	29.241	34.292	37.664

If for a given layer each hour had a standard deviation above 20, then that layer was determined to be the cut-off layer. This value was chosen because there is a 20ppb difference between categories in the EPA's Air Quality Index (AQI) (U.S. EPA, 1999). The AQI is the standard index used to report current and future ozone concentrations. It was deemed that if the variation was greater than one AQI category, it was too large. Standard deviations of 20 or larger at each hour began to occur at layer H, or at 2400m. Because of this, NEXLASER data at and above this layer was not considered in succeeding analysis.

To examine the potential relationship seen in Figure 6 between the upper-tropospheric ozone concentrations and surface maximums, layers below 2400m were correlated with each of the afternoon surface 8-hour ozone maximums. The R-squared values of this analysis are shown in Table 6.

Table 6: Correlations between upper-tropospheric ozone and surface 8-hour ozone maximums.

METRO							
Layer (m)	6AM	7AM	8AM	9AM	10AM	11AM	NOON
G	0.061	0.000	0.504	0.479	0.419	0.387	0.075
F	0.181	0.200	0.178	0.464	0.433	0.503	0.416
E	0.082	0.150	0.097	0.381	0.377	0.270	0.321
D	0.319	0.260	0.271	0.355	0.378	0.515	0.356
C	0.261	0.220	0.165	0.255	0.240	0.361	0.305
B	0.203	0.120	0.066	0.256	0.189	0.131	0.175
A	0.291	0.060	0.037	0.064	0.090	0.057	0.570
AVERAGE							
Layer (m)	6AM	7AM	8AM	9AM	10AM	11AM	NOON
G	0.036	0.000	0.518	0.548	0.448	0.433	0.074
F	0.138	0.240	0.188	0.505	0.430	0.561	0.463
E	0.052	0.140	0.102	0.393	0.397	0.283	0.352
D	0.289	0.280	0.287	0.372	0.404	0.542	0.366
C	0.216	0.230	0.173	0.263	0.249	0.372	0.304
B	0.308	0.160	0.074	0.252	0.166	0.136	0.178
A	0.394	0.080	0.043	0.058	0.082	0.052	0.579
LOCAL							
Layer (m)	6AM	7AM	8AM	9AM	10AM	11AM	NOON
G	0.049	0.000	0.434	0.439	0.383	0.362	0.089
F	0.187	0.160	0.158	0.436	0.369	0.463	0.369
E	0.050	0.090	0.064	0.311	0.318	0.227	0.306
D	0.245	0.200	0.226	0.293	0.318	0.454	0.285
C	0.223	0.190	0.138	0.199	0.184	0.287	0.246
B	0.240	0.120	0.061	0.192	0.152	0.099	0.174
A	0.234	0.060	0.037	0.039	0.047	0.034	0.544

As seen, there is a varying magnitude to these numbers. However, these correlations are comparable to those of such ozone predictor variable as temperature and wind speed

(Davis and Speckman, 1999). While no conclusive patterns can be discerned, a few important observations can be made. First, higher correlations mainly occurred in the later hours. Second, the higher correlations generally occurred above 900m. This later observation suggests that the ozone at the appropriate height of a residual layer does have important influence as it mixes with the newly formed ozone from the surface. Third, the correlations were usually higher when considering the average 8-hour maximum concentration. The difference is not large, but fairly consistent. This makes sense when considering that specific sites can be influenced by local phenomenon unrelated to the upper-tropospheric ozone.

It is important to note that these correlations are based on average values. As with other forecasting variables, the significance of any influence will vary depending on the circumstances. Thus, it is of interest to examine specific days in detail.

CHAPTER 4

CASE STUDIES

As stated previously, there is a need to examine a few specific periods in more detail. It is of interest to study a couple of periods that contain days with high and low ozone concentrations. Ideally, there has to be a high ozone day in the middle of the series with relatively low ozone days before and after. This will allow for examination of the differences between the days leading to the extreme event through the following day.

Figure 7 shows the metropolitan Atlanta's daily maximum 8-hour average ozone concentration for each day through the study period. Days which have NEXLASER data are colored in blue.

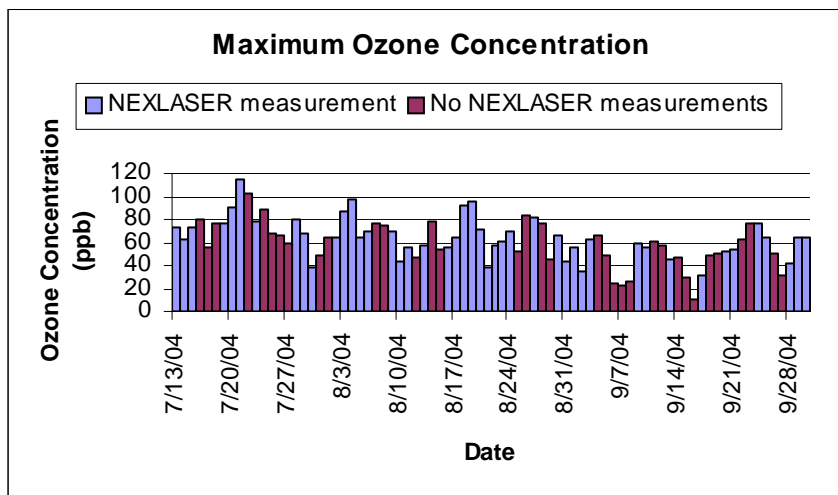


Figure 7: Metropolitan Atlanta's daily maximum ozone concentration

From Figure 7, the days that have maximum ozone concentrations above the EPA standard (84ppb) are 20, 21, 22 and 24 July and 3, 4, 18 and 19 August. Of these dates, only those in August have NEXLASER data for both the extreme days and those before

and after the event. In order to examine the relatively low ozone days before and after the high concentration days, the case studies examined were 2 August through 5 August and 17 August through 20 August.

To study these two periods, meteorological variables were looked at along with the NEXLASER and hourly mixing height charts. The meteorological data was retrieved from NOAA's Air Resource Laboratory in the form a EDAS (ETA Data Assimilation System) 40 Meteogram (NOAA, 2005). These meteograms contain 3-hour archived ETA data for wind, temperature, surface pressure, and cloud coverage at a 40km resolution around Atlanta. This resolution is appropriate because it allows for a general representation of the study region and not just one point location. The meteograms also contain 3-hour average precipitation totals. The hours for this data are represented in UTC.

Along with the meteograms and NEXLASER charts, the slope of the ozone increase for each day was inspected. This slope was calculated by taking the change in ozone concentration from the start of the increase in the morning to the afternoon maximum and dividing it by the change in time. This value was calculated for each monitoring site for each day. Those sites that did not have afternoon ozone measurements for that day were marked as non-applicable (N/A). The slope was determined to observe if there was a change in the rate at which 8-hour average ozone increased. If this rate of change increased, it could indicate the influence of a reservoir layer.

Case 1: 2 August through 5 August

To begin examining this case study, meteograms, the NEXLASER charts, and the slopes of ozone increase for each day were gathered. Figure 8, Figure 9, Figure 10 and Figure 11 contain the four meteograms. Figure 12 contains the NEXLASER charts. Table 7 contains the ozone slopes along with the maximum 8-hour average ozone per monitoring site.

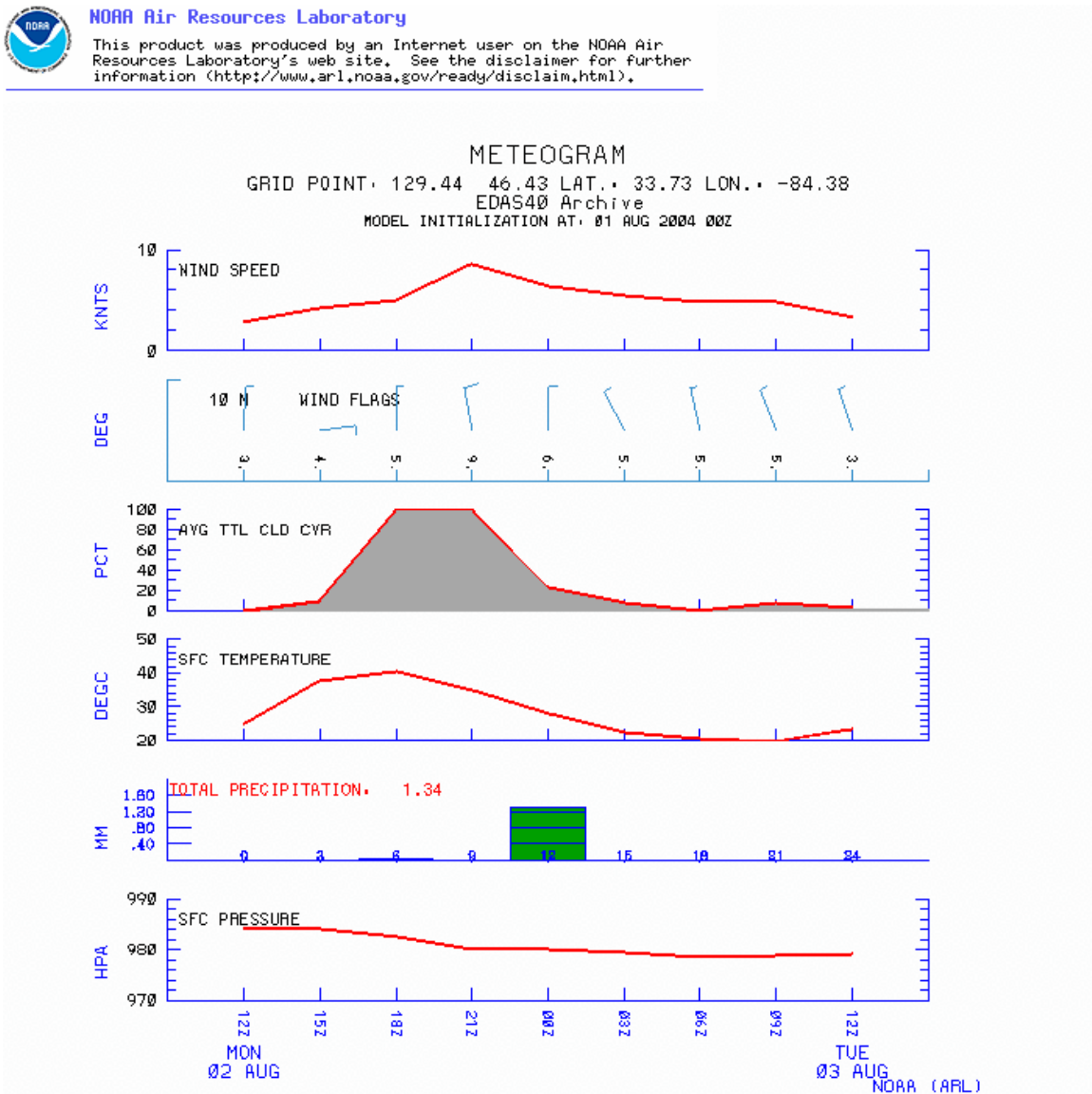


Figure 8: 2 August Meteogram (NOAA, 2005)



NOAA Air Resources Laboratory

This product was produced by an Internet user on the NOAA Air Resources Laboratory's web site. See the disclaimer for further information (<http://www.arl.noaa.gov/ready/disclaim.html>).

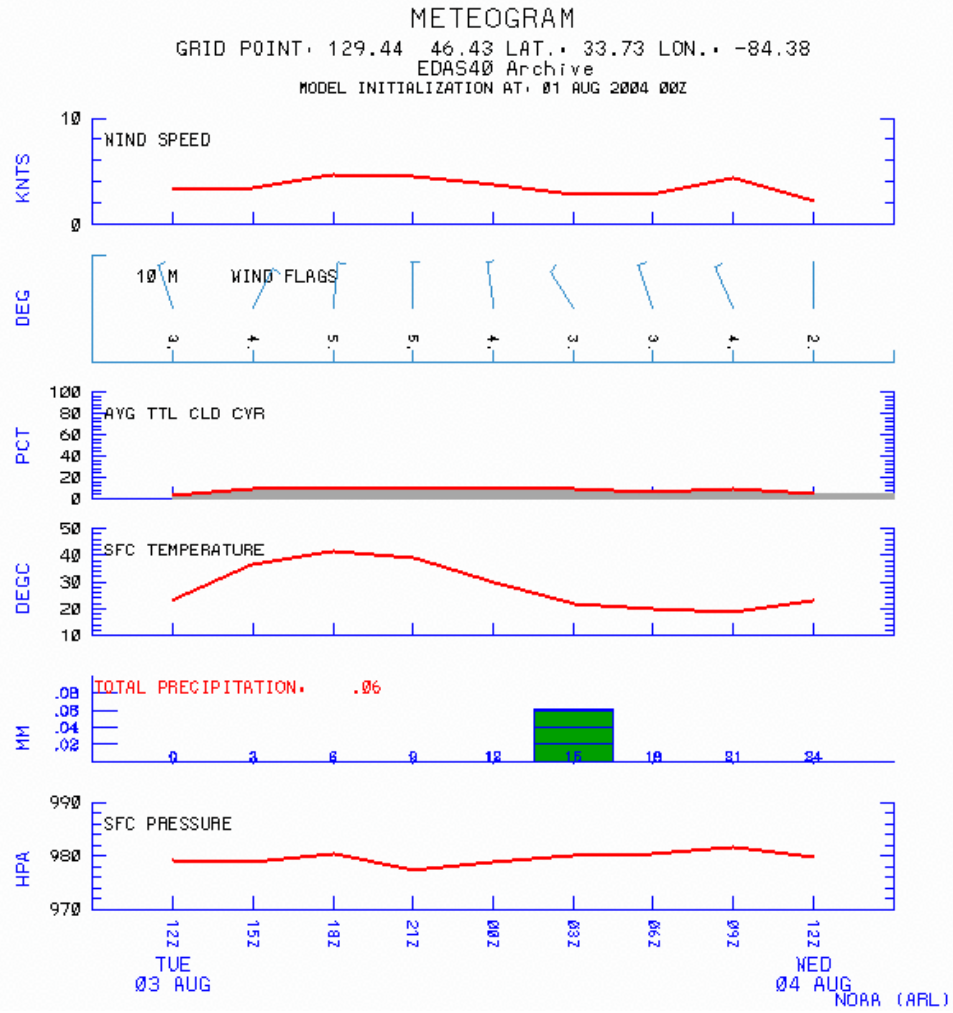


Figure 9: 3 August Meteogram (NOAA, 2005)



NOAA Air Resources Laboratory

This product was produced by an Internet user on the NOAA Air Resources Laboratory's web site. See the disclaimer for further information (<http://www.arl.noaa.gov/ready/disclaim.html>).

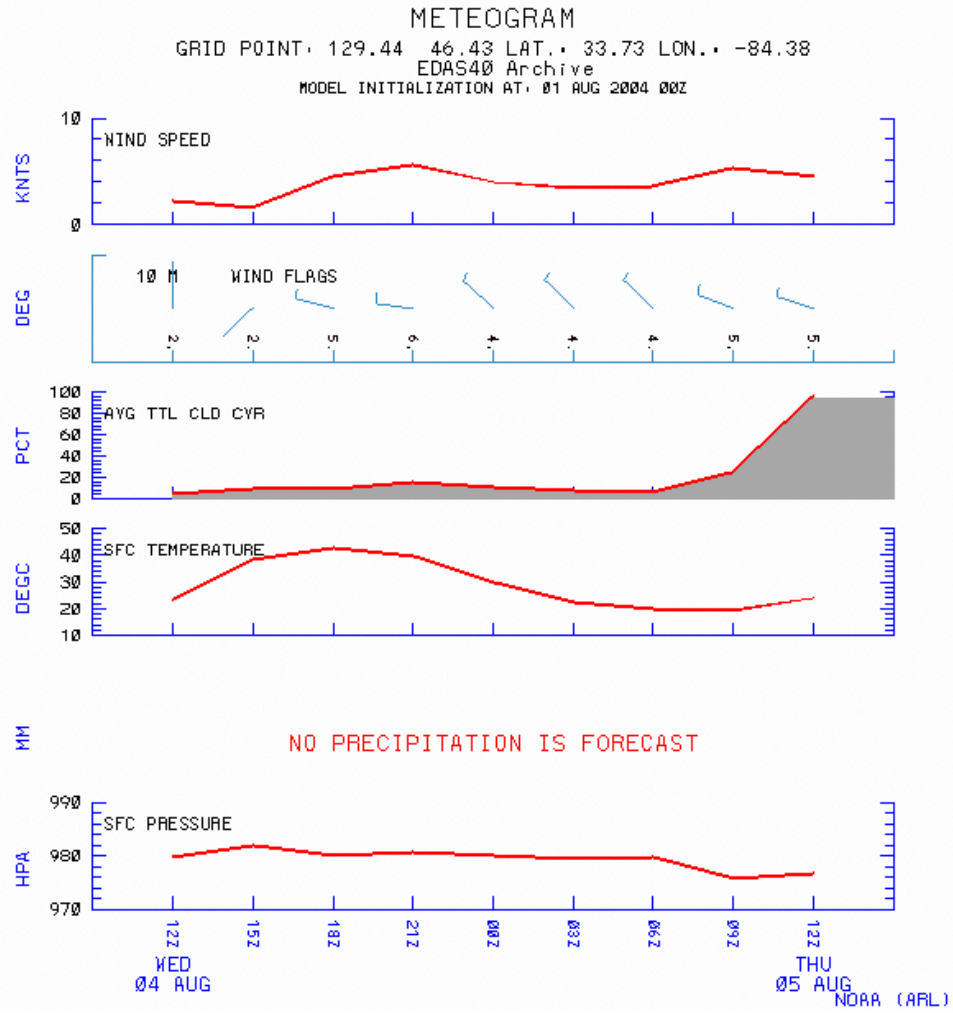


Figure 10: 4 August Meteogram (NOAA, 2005)



NOAA Air Resources Laboratory

This product was produced by an Internet user on the NOAA Air Resources Laboratory's web site. See the disclaimer for further information (<http://www.arl.noaa.gov/ready/disclaim.html>).

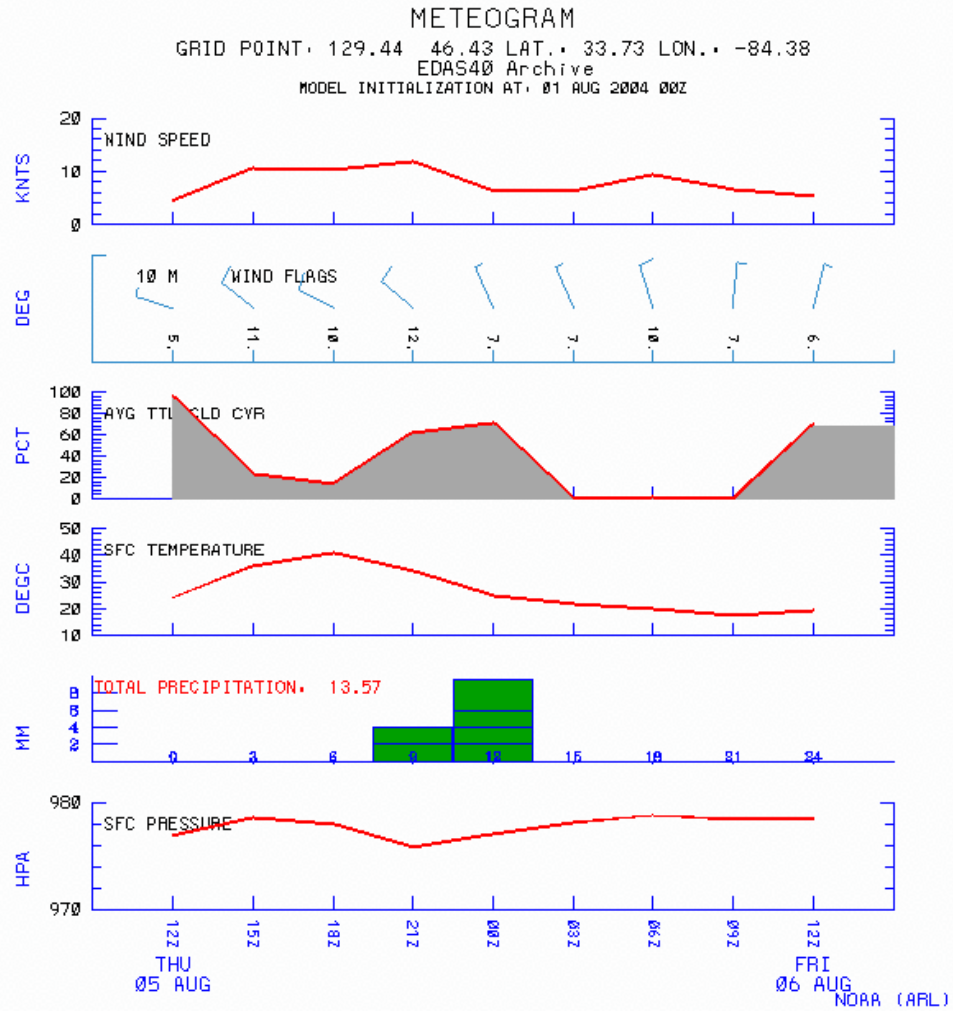
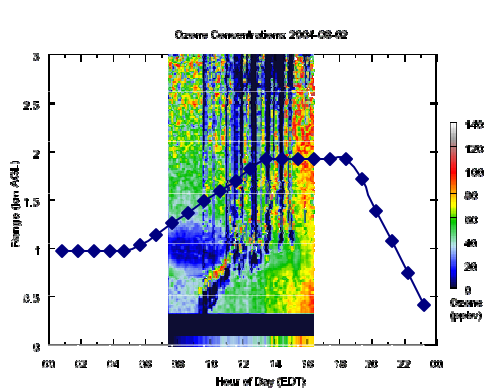
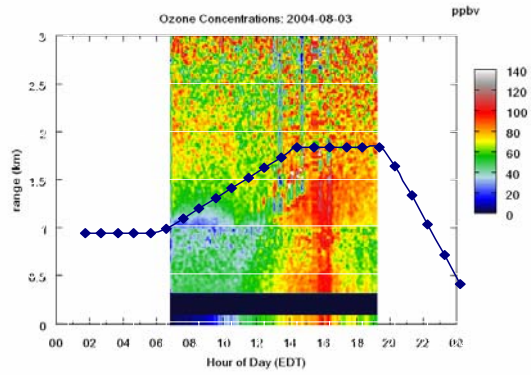


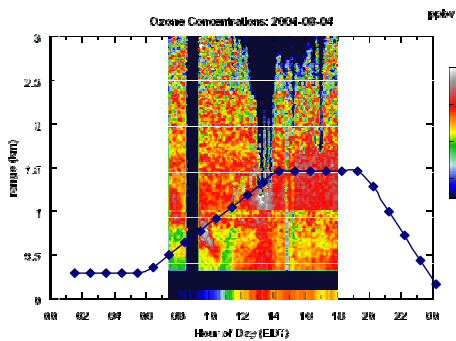
Figure 11: 5 August Meteogram (NOAA, 2005)



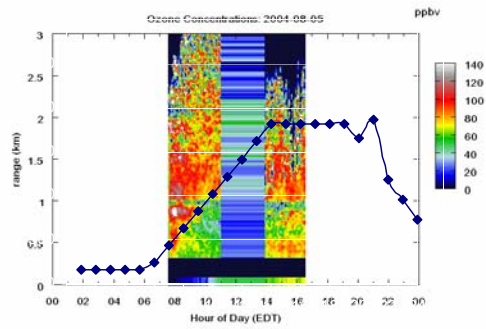
2 August



3 August



4 August



5 August

Figure 12: NEXLASER and hourly mixing height charts for 2 August through 5 August

Table 7: Maximum 8-hour average ozone per monitoring site and rate of ozone increase

Maximum Ozone (ppb)				
	2-Aug	3-Aug	4-Aug	5-Aug
SDEKALB	43.0	72.0	86.0	56.0
CONYERS	46.0	70.0	90.0	63.0
CONFDAVE	54.0	73.0	86.0	57.0
TUCKER	41.0	59.0	88.0	N/A
GWINNETT	45.0	59.0	97.0	53.0
YORKVILL	52.0	62.0	62.0	54.0
DOUGLASV	58.0	66.0	N/A	55.0
FAYETTVL	64.0	77.0	78.0	63.0
MCDNOUGH	58.0	87.0	82.0	65.0
NEWNAN	57.0	63.0	76.0	65.0
KENNESAW	54.0	56.0	68.0	46.0
average	52.0	67.6	81.3	57.7
Rate of Ozone Increase (ppb/hr)				
	2-Aug	3-Aug	4-Aug	5-Aug
SDEKALB	4.7	6.2	8.5	6.1
CONYERS	3.8	5.9	9.9	7.0
CONFDAVE	5.4	4.2	8.5	5.7
TUCKER	3.9	5.2	7.7	N/A
GWINNETT	3.4	6.1	8.5	5.9
YORKVILL	3.1	4.2	4.0	2.6
DOUGLASV	4.3	4.1	N/A	1.4
FAYETTVL	5.5	6.1	7.7	6.2
MCDNOUGH	4.5	6.1	7.4	6.5
NEWNAN	4.5	4.5	6.5	4.3
KENNESAW	4.7	5.4	6.6	3.0
average	4.3	5.3	7.5	4.9

To begin, let's look at the 2 August and 3 August. As seen in Table 7, the average 8-hour maximum ozone concentration increased, along with the average rate of increase in ozone concentrations. Examining the meteorograms in Figure 8 and Figure 9 shows how the hourly wind speed, direction and temperature fluctuations were similar for both days. The main difference was the amount of cloud coverage and precipitation. 2 August had more cloud coverage and more accumulated precipitation. The NEXLASER plots for 2 August and 3 August in Figure 12 do not indicate that there were high concentrations of ozone in the reservoir layer in the early-morning upper boundary layer for either day.

On 4 August, the average 8-hour maximum ozone concentration is higher than on 3 August. Ozone also increased at a steeper rate at most monitoring sites. Consulting the 4 August meteorogram in Figure 10 shows how most of the meteorological variables are similar to those on 3 August during the morning and afternoon hours. The main difference is that there is no precipitation on 4 August. When the NEXLASER chart for 4 August is examined, an early morning high ozone concentration layer can clearly be seen.

On 5 August, the 8-hour maximum ozone concentrations at each monitoring sites decreased. After examining the meteorogram in Figure 11, it was determined that the meteorological conditions were most similar to those of 2 August. This was primarily due to the increased amount of clouds and precipitation. Though, 5 August had a larger precipitation total. However, for most sites, the maximum 8-hour ozone concentrations were higher than those on 2 August. Also, the rate of ozone increase at most sites was larger than those on 2 August. Examining the 5 August NEXLASER chart shows how there is a reservoir layer in the morning.

Case 2: 17 August through 20 August

As with the previous case study, meteograms, the NEXLASER charts, and the slopes of ozone increase for each day were gathered. Figure 13, Figure 14, Figure 15 and Figure 16 contain the four meteograms. Figure 16 contains the NEXLASER charts. Table 8 contains the rate of ozone increase along with the maximum 8-hour average ozone per monitoring site.

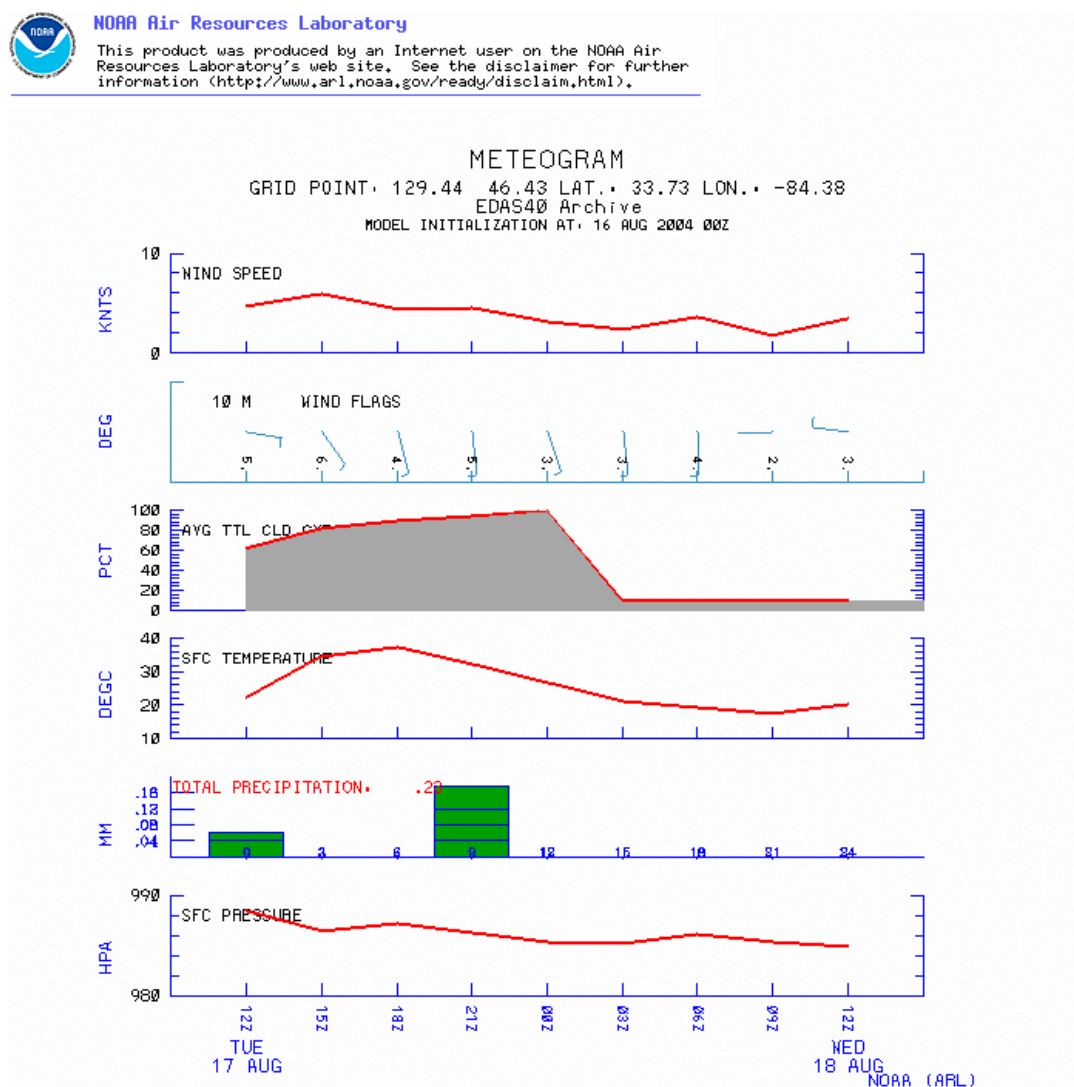


Figure 13: 17 August Meteogram (NOAA, 2005)



NOAA Air Resources Laboratory

This product was produced by an Internet user on the NOAA Air Resources Laboratory's web site. See the disclaimer for further information (<http://www.arl.noaa.gov/ready/disclaim.html>).

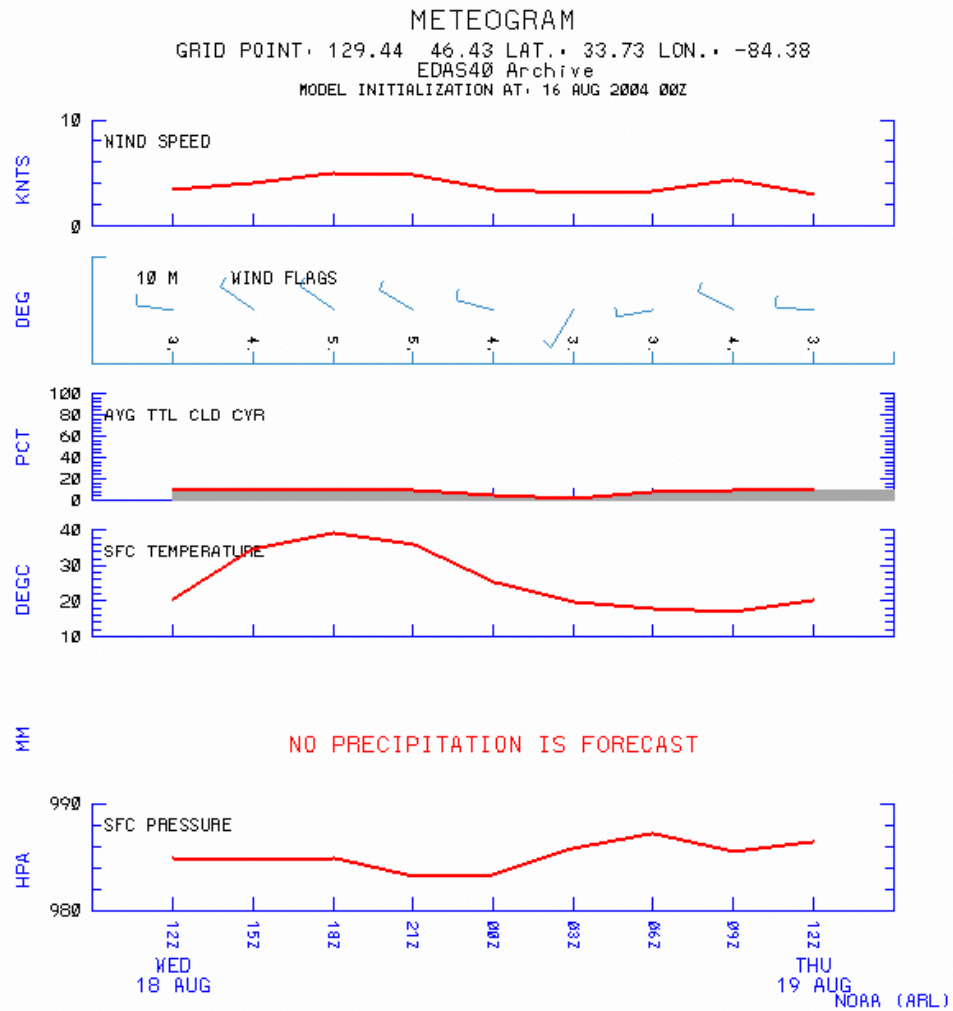


Figure 14: 18 August Meteogram (NOAA, 2005)



NOAA Air Resources Laboratory

This product was produced by an Internet user on the NOAA Air Resources Laboratory's web site. See the disclaimer for further information (<http://www.arl.noaa.gov/ready/disclaim.html>).

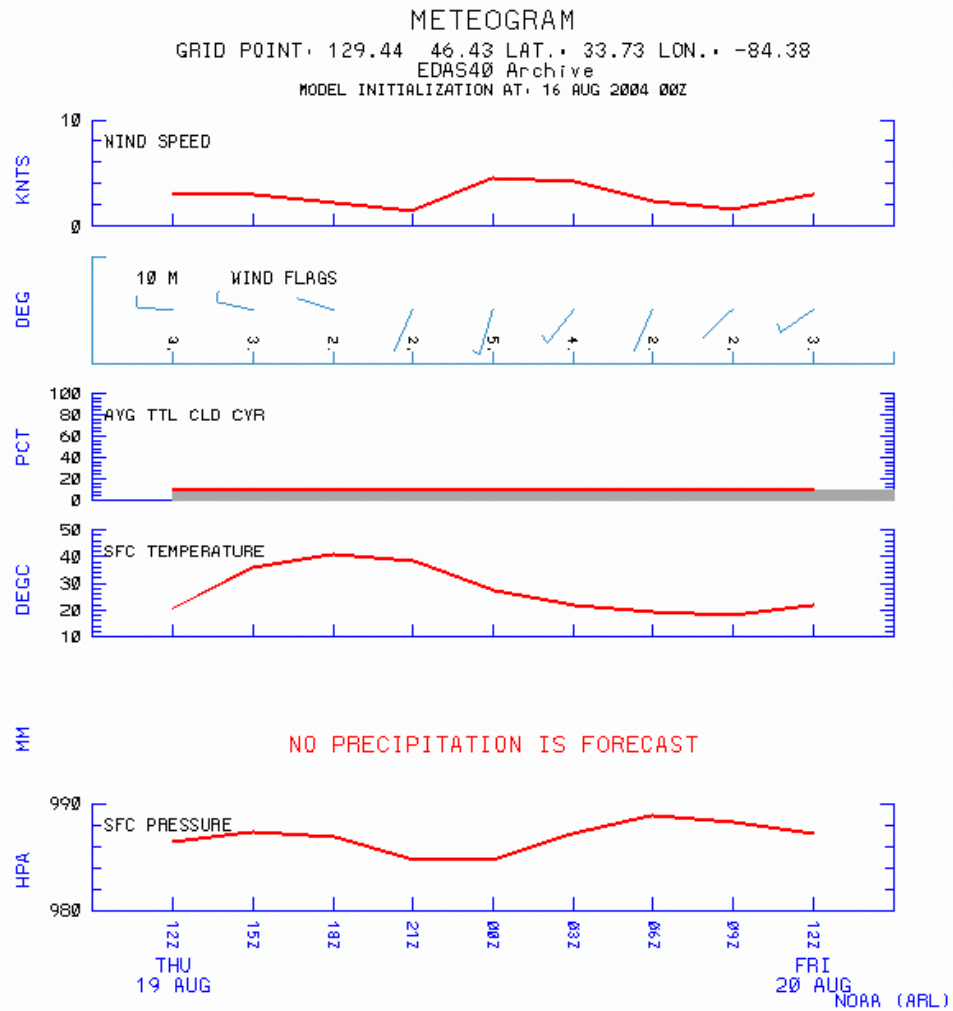


Figure 15: 19 August Meteogram (NOAA, 2005)



NOAA Air Resources Laboratory

This product was produced by an Internet user on the NOAA Air Resources Laboratory's web site. See the disclaimer for further information (<http://www.arl.noaa.gov/ready/disclaim.html>).

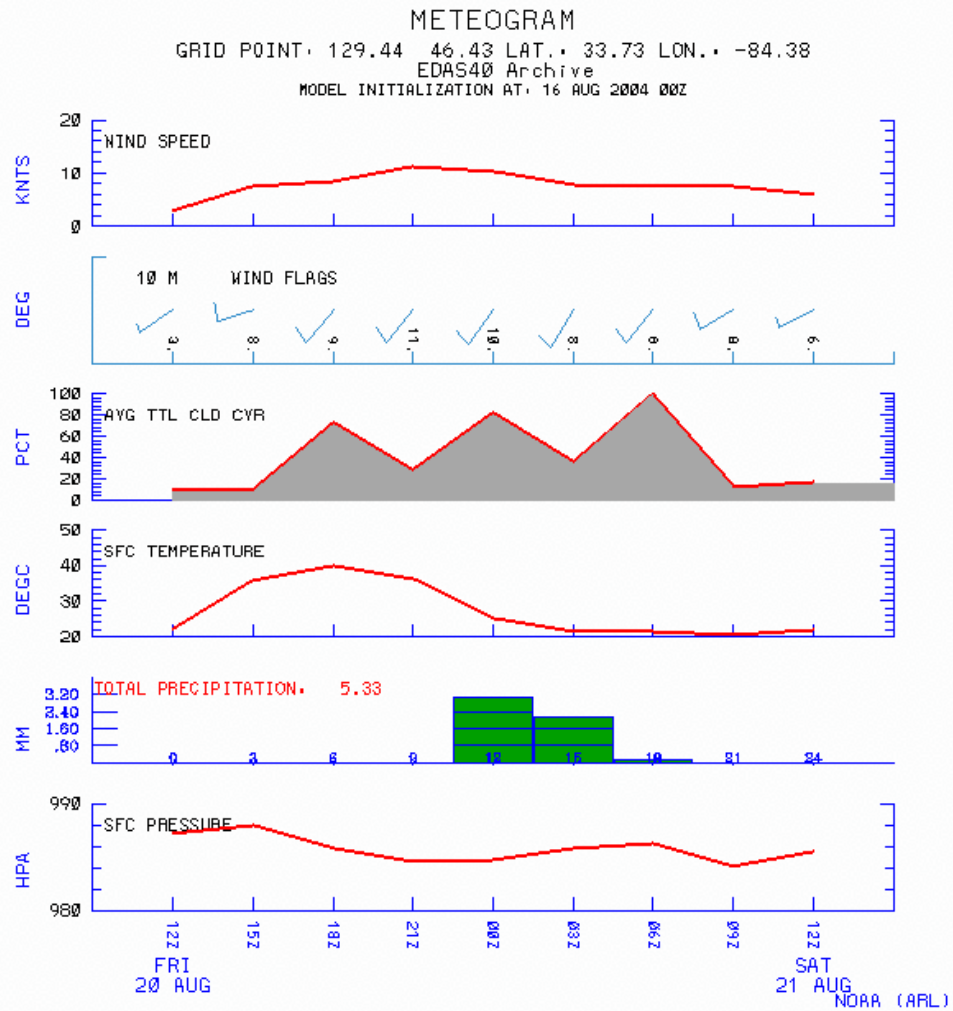
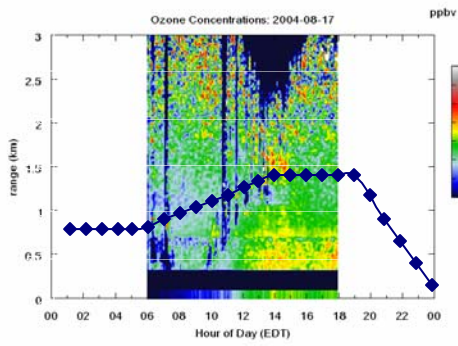
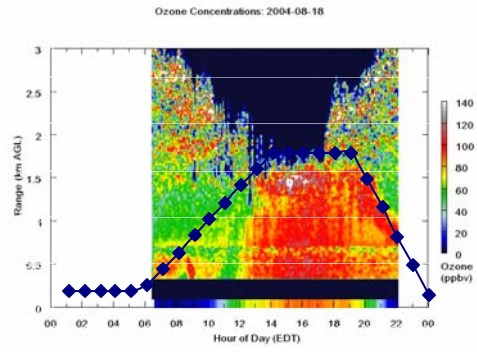


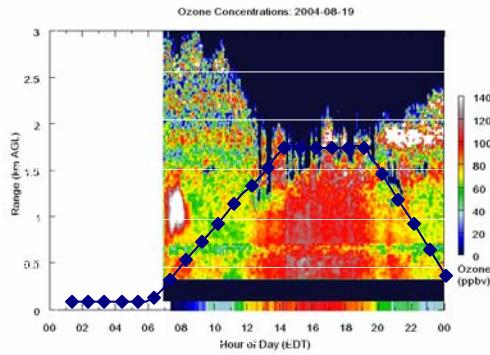
Figure 16: 20 August Meteogram (NOAA, 2005)



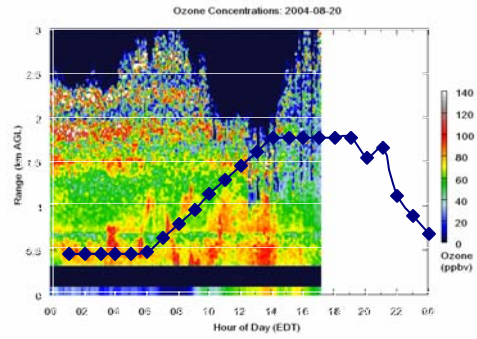
17 August



18 August



19 August



20 August

Figure 17: NEXLASER and hourly mixing height charts for 17 August through 20 August

Table 8: Maximum 8-hour average ozone per monitoring site and rate of ozone increase

Maximum Ozone (ppb)				
	17-Aug	18-Aug	19-Aug	20-Aug
SDEKALB	49.0	82.0	88.0	57.0
CONYERS	44.0	81.0	87.0	58.0
CONFDAVE	63.0	90.0	96.0	64.0
TUCKER	58.0	N/A	89.0	61.0
GWINNETT	65.0	79.0	80.0	71.0
YORKVILL	45.0	67.0	N/A	41.0
DOUGLASV	45.0	N/A	72.0	N/A
FAYETTVL	N/A	79.0	82.0	52.0
MCDNOUGH	44.0	93.0	87.0	55.0
NEWNAN	43.0	73.0	84.0	37.0
KENNESAW	47.0	73.0	70.0	49.0
average	50.3	79.7	83.5	54.5
Rate of Ozone Increase (ppb/hr)				
	17-Aug	18-Aug	19-Aug	20-Aug
SDEKALB	5.3	7.4	9.7	7.0
CONYERS	4.4	7.3	8.7	7.1
CONFDAVE	5.5	7.9	8.2	6.4
TUCKER	5.4		8.1	6.2
GWINNETT	5.4	7.5	8.0	7.1
YORKVILL	3.7	4.8	N/A	2.1
DOUGLASV	3.2	N/A	2.8	N/A
FAYETTVL	N/A	7.3	8.1	5.8
MCDNOUGH	3.7	7.8	8.6	5.6
NEWNAN	3.9	5.1	6.2	4.5
KENNESAW	4.6	7.7	6.4	5.4
average	4.5	7.0	7.5	5.7

As with the previous case study, the first two days of the period were examined first. As seen in Table 8, the 8-hour maximum ozone concentration increased on 18 August at every monitoring site, along with the average rate of increase in ozone concentrations. Examining the meteograms in Figure 13 and Figure 14 for those two days shows how the hourly wind speeds were similar, but the direction shifted from predominately southerly flow to westerly. The temperature fluctuations were also similar. The main difference was the larger amount of cloud coverage on 17 August and the minor precipitation accumulation. Also, the NEXLASER plots in Figure 17 indicate that while there were no high concentrations of ozone in the reservoir layer in the early morning upper boundary layer for 17 August, there was some on 18 August.

On 19 August, the average 8-hour maximum ozone concentration is higher than on 18 August. Ozone also increased at a more rapid rate at most monitoring sites. Consulting the 19 August meteogram in Figure 15 shows how most of the meteorological variables are similar to those on 18 August. The main difference is that the wind direction shifted back to the South- Southwest. When the NEXLASER chart for 19 August was examined, an early morning high ozone concentration layer can clearly be seen.

On 20 August, the 8-hour maximum ozone concentrations at each monitoring site decreased. After examining the meteogram in Figure 16, it was determined that the meteorological conditions were most similar to those of 17 August. This was primarily due to the increased amount of clouds and precipitation. Though, 20 August had a larger precipitation total and the winds were stronger. However, for most sites, the maximum 8-hour ozone concentrations were higher than those on 17 August. Also, the rate of ozone

increase at most sites was larger than those on 17 August. Examining the 20 August NEXLASER chart shows how that there is a reservoir layer in the morning.

CHAPTER 5

CONCLUSION

The main objective of this study was to evaluate NEXLASER to determine if it can be used to detect the presence of residual layers and if it can be used as an aid in predicting peak daily ground-level ozone concentrations. When looking at the NEXLASER charts with the hourly mixing heights overlaid, residual layers can be seen and the potential influence on afternoon surface concentrations can be suggested. Correlations between the hourly morning upper-tropospheric ozone concentrations and the afternoon 8-hour surface maximum concentration confirm that there are relationships. While the R^2 values are not large, they do indicate that the morning ozone concentrations aloft do have some influence over the afternoon surface maximums. When examining a few days in detail, this influence can be further suggested through noted increases in the afternoon surface maximum concentrations and the rate at which this ozone increases throughout the afternoon on days when morning ozone concentrations aloft were high.

This study shows how the measured morning ozone concentrations from NEXLASER relate to maximum afternoon surface concentrations and how the ozone reservoir layer can potentially influence high afternoon surface concentrations. There still needs to be further research done using more days and different seasons, but this study does indicate potential. It is very important for forecasters to accurately predict extreme ozone events. Being able to further explain why extreme ozone events occur on certain days will aid these forecasters. This study suggests that utilizing morning upper-boundary layer ozone concentrations and identifying potential reservoir layers could be an important tool.

REFERENCES

- Arya S. Pal. (1999) Air Pollution Meteorology and Dispersion. Oxford University Press, Inc. 59.
- Baumbach Gunter and Vogt Ulrich. (2003) Influence of Inversion Layers on the Distribution of Air Pollution in Urban Areas. *Water, Air, and Soil Pollution: Focus* **3**, 65-76.
- Braur Michael and Brook Jeffrey R.. (1997) Ozone Personal Exposures and Health Effects for Selected Groups Residing in the Fraser Valley. *Atmospheric Environment* **31**(14), 2113-2121.
- Brunekreef Bert and Holgate Stephen T. (2002) Air Pollution and Health. *The Lancet* **360**, 1233-1242.
- Comrie Andrew C. and Yarnal Brent. (1991) Relationships Between Synoptic-Scale Atmospheric Circulation and Ozone Concentrations in Metropolitan Pittsburgh, Pennsylvania. *Atmospheric Environment* **26B**, 301-312.
- Cox William M. and Chu Shao-Hang. (1993) Meteorologically Adjusted Ozone Trends in Urban Areas: A Probabilistic Approach. *Atmospheric Environment* **27B**(4), 425-434.
- Davis, J.M and P. Speckman.(1999) A model for predicting maximum and 8h average ozone in Houston. *Atmospheric Environment* **33** 2487-2500.
- Federal Register. (1997) National Ambient Air Quality Standards for Ozone: Final Rule 40 CFR Part 50, July 18, 1997. *Federal Register* **62**(138), 1.
- Federal Register. (2003) National Ambient Air Quality Standards for Ozone: Final Response to Remand; Rule 40 CFR Part 50, January 6, 2003. *Federal Register* **68**(3), 1.
- Fredriksson, Kent A. and Hans M. Hertz. (1984) Evaluation of the DIAL technique for studies on NO₂ using a mobile lidar system. *Applied Optics* **23**(9) 1403-1411.
- Frischer T, Studnicka M., Halmerbauer G., Horak F. Jr., Gartner C., Tauber E., and Koller D. Y.. (2001) Ambient Ozone Exposure is Associated with Eosinophil Activation in Healthy Children. *Clinical and Experimental Allergy* **31** 1213-1219.
- Gimmestad Gary G.. (2005) Lidar: Range-Resolved Optical Remote Sensing of the Atmosphere. Chapter 7: Differential-absorption lidar for ozone and industrial emissions.

- Gimmestad, Gary G., E.M. Patterson, D.W. Roberts, J.W. Stewart, L.L West, and J.W. Wood. (2001) A Next-Generation Ground-Based Sensor for Tropospheric Ozone. *Proc. IEEE Int.Geosci. Remote Sensing Symposium* 1-3.
- Gong Henry Jr, McManus Michael S. and Linn William S..(1997) Attenuated Response to Repeated Daily Ozone Exposures in Asthmatic Subjects. *Archives of Environmental Health* **52**(1), 34-41.
- Govett Mark. (2004) FSL/NCDC Radiosonde Database Access. National Oceanic and Atmospheric Administration (October 2004). <<http://roab.fsl.noaa.gov>>.
- Guicherit Robert and Roemer Michiel. (2000) Tropospheric Ozone Trends. *Chemosphere-Global Change Science* **2**, 167-183.
- Hayden K.L, Anlauf K.G., Hoff R.M., Strapp J.W., Bottenheim J.W., Wiebe H.A., Froude F.A., Martin J.B., Steyn D.G and McKendry I.G. (1997) The Vertical Chemical and Meteorological Structure of the Boundary Layer in the Lower Fraser Valley During Pacific '93. *Atmospheric Environment* **31**(14), 2089-2105.
- Jacob Daniel J. (1999) Introduction to Atmospheric Chemistry. Princeton University Press. 200-219,231-241.
- Jorres Rudolf A., Holz Olaf, Zachgo Wolfgang, Timm Petra, Koschyk Silke, Muller Bernd, Grimminger Friedrich, Seeger Werner, Kelly Frank J., Dunster Christine, Frischer Thomas, Lubec Gerd, Waschewski Marc, Niendorf Axel and Magnussen Helgo. (2000) The Effect of Repeated Ozone Exposures on Inflammatory Markers in Bronchoalveolar Lavage Fluid and Mucosal Biopsies. *American Journal of Respiratory and Critical Care Medicine* **161**, 1855-1861.
- Kinney Patrick L and Lippmann Morton. (2000) Respiratory Effects of Seasonal Exposures to Ozone and Particles. *Archives of Environmental Health* **55**(3), 210-216.
- Ludwig F.L., Jiang Jih-Yih and Chen Jun. (1995) Classification of Ozone and Weather Patterns Associated with High Ozone Concentrations in the San Francisco and Monterey Bay Areas. *Atmospheric Environment* **29**(21), 2915-2928.
- National Climatic Data Center (2005) Dynamically Regenerated Unedited Local Climatic Data (November 2004). <<http://cdo.ncdc.noaa.gov/ulcd/ULCD>>.
- National Oceanic and Atmospheric Administration. (2004) Archived Meteorology. Air Resources Laboratory: READY (February 2005). <<http://www.arl.noaa.gov/ready/amet/html>>.
- Pryor, S.C. and D.G. Steyn. (1995) Hebdomadal and diurnal cycles in ozone time series

- from the Lower Fraser Valley, B.C.. *Atmospheric Environment* **29**(9), 1007-1019.
- Sasano, Yasuhiro, Edward V. Browell, and Syed Ismail. (1985) Error caused by using a constant extinction/backscattering ratio in the lidar solution. *Applied Optics* **24**(22) 3929-3932.
- Seinfeld John H. and Pandis Spyros N..(1998) *Atmospheric Chemistry and Physics: From Air Pollution to Climate Change*. Wiley-Interscience Publications. 254-262, 296-300.
- Sica, R. (1999) Exploring the Atmosphere with Lidars. The Department of Physics and Astronomy: University of Western Ontario (January 2005). <<http://pcl.physics.uwo.ca/pclhtml/introlidar/introlidar.html>>.
- Stewart, John M., Gary G. Gimmestad, David W. Roberts, Leanne L. West, and Jack Wood. (2002) NEXLASER-An unattended tropospheric aerosol and ozone lidar. *Laser Radar Technology and Applications VII* **4723** 172-181.
- Thurston George D. and Ito Kazuhiko. (2001) Epidemiological Studies of Acute Ozone Exposures and Mortality. *Journal of Exposure Analysis and Environmental Epidemiology* **11**, 286-294.
- U.S. Environmental protection Agency (U.S. EPA). (1990) Users Guide for the Urban Airshed Model. EPA-450/4-90-007B. Office of Air Quality Planning and Standards, Research Triangle, NC .
- U.S. Environmental Protection Agency (U.S. EPA). (1996) Air Quality Criteria for Ozone and Other Photochemical Oxidants. EPA-600/P-93/004aF Executive Summary. Environmental Criteria and Assessment Office, Research Triangle Park, NC.
- U.S. Environmental Protection Agency (U.S. EPA). (1999) Guideline for Reporting of Daily Air Quality – Air Quality Index (AQI). EPA-454/R-99-010. Office of Air Quality Planning and Standards, Research Triangle, NC. 1-17.
- U.S. Environmental Protection Agency (U.S. EPA) (1999) PCRAMMET User’s Guide. EPA-454/B-96-001. Meteorological Preprocessors. Technology Transfer Network Support Center for Regulatory Air Models (November 2004). <<http://www.epa.gov/scram001/tt24.htm#preps>>.
- U.S. Environmental Protection Agency (U.S. EPA) (2005) Meteorological Preprocessors. Technology Transfer Network Support Center for Regulatory Air Models (November 2004). <<http://www.epa.gov/scram001/tt24.htm#preps>>.
- Vaughan,G. (2003) Atmospheric Physics: LIDAR. The Department of Physics: University of Wales, Aberystwyth (January 2005). <<http://users.aber.ac.uk/ozone/lidar.html>>.

Weibring, Peter, Hans Edner, and Sune Svanberg. (2003) Versatile mobile lidar System for environmental monitoring. *Applied Optics* **42**(18) 3583-3594.

Zimmer-Dauphinee, Susan. (2005) Ambient Monitoring Program Database Query. Air Monitoring Program (October 2004). <http://www.air.dnr.state.ga.us/amp/amp_query.html>.